coatings

MDPI

Article

Investigation of Factors Affecting the Intermediate-Temperature Cracking Resistance of In-Situ Asphalt Mixtures Based on Semi-Circular Bending Test

Duo Xu [1], Fujian Ni [1,*], Hui Du [2], Zili Zhao [1], Jingling Wang [1] and Sheng Chen [3]

[1] School of Transportation, Southeast University, Nanjing 211189, China
[2] School of Civil Engineering, Fujian University of Technology, Fuzhou 350118, China
[3] Huai'an Boyan Civil Engineering Research Institute Co., Ltd., Huai'an 223003, China
* Correspondence: 101004746@seu.edu.cn

Abstract: Cracking is one of the main distresses in asphalt pavement. At present, few studies have been conducted on the cracking performance of asphalt mixtures from the field due to the difficulty of sample collection. Therefore, this study aims to assess the cracking resistance of in-service asphalt pavement at intermediate temperature using a large number of field cores in Jiangsu province, China. A semi-circular bending (SCB) test at 25 °C was conducted on field-cored samples covering three asphalt layers from 16 in-service road sections that represent a combination of influencing factors, including air void, mixture type, service age, cumulative number of equivalent single-axle loads (ESALs), and overload rate. The flexibility index (FI) and tensile strength were calculated from the experimental data as cracking performance evaluation indices. According to the analysis of variance results, at the top layer, ESALs and service age had a strong influence on cracking resistance. The decline rate of FI became slower with increasing ESALs. The most rapid decline in crack resistance with service age occurred on medium-traffic-level sections that served for over 14 years. At the middle layer, the overload rate replaced service age as a significant factor for FI. At the bottom layer, the air void was the only significant factor affecting the cracking resistance. In general, as the depth of layer increased, the effect of traffic load and service age decreased, whereas the effect of material properties increased. In addition, the FI and tensile strength were more sensitive to traffic load and air void, respectively.

Keywords: cracking resistance; intermediate temperature; semi-circular bending test; influencing factors; different asphalt layers

check for updates

Citation: Xu, D.; Ni, F.; Du, H.; Zhao, Z.; Wang, J.; Chen, S. Investigation of Factors Affecting the Intermediate-Temperature Cracking Resistance of In-Situ Asphalt Mixtures Based on Semi-Circular Bending Test. *Coatings* **2023**, *13*, 384. https://doi.org/10.3390/coatings13020384

Academic Editors: Valeria Vignali and Joaquim Carneiro

Received: 27 December 2022
Revised: 4 February 2023
Accepted: 5 February 2023
Published: 7 February 2023

Copyright: © 2023 by the authors. Licensee MDPI, Basel, Switzerland. This article is an open access article distributed under the terms and conditions of the Creative Commons Attribution (CC BY) license (https://creativecommons.org/licenses/by/4.0/).

1. Introduction

Cracking is one of the major challenges experienced by asphalt pavements. The major cracking distresses in asphalt pavements can be categorized into reflection cracking, thermal cracking, and fatigue cracking [1]. Field fatigue cracking is caused by tensile stress concentrations produced by repeated traffic loads at intermediate temperatures. The presence of cracks increases the surface roughness, resulting in reduced ride quality and an increased risk of traffic accidents [2]. Without timely and appropriate maintenance or rehabilitation of the asphalt layer, cracking will result in severe performance degradation and the premature failure of pavements [3]. Therefore, to make reasonable rehabilitation decisions, it is important to assess the resistance to intermediate-temperature cracking of existing asphalt mixtures from in-service pavements.

Various testing methods have been proposed to characterize the cracking resistance of asphalt mixtures. These include the indirect tension (IDT) test [4,5], single-edge notch beam (SENB) test [6,7], disk-shaped compact tension (DCT) test [8], overlay test (OT) [9,10], Fenix test [11], dog-bone direct tension (DBDT) test [12], indirect tensile asphalt cracking test (IDEAL-CT) [13], and semicircular bending (SCB) test [3,14,15]. The pros and cons of

each method and performance index were determined in many aspects [16–18]. As it is simple, reliable, and reproducible, the SCB test has drawn attention from researchers and was selected for this study to assess the cracking resistance of asphalt mixtures from field cores at intermediate temperatures. The SCB test uses monotonic loading at a constant rate and records a load–displacement curve for further evaluation [19]. Among the several different SCB testing modes, the semi-circular bending Illinois flexibility index (SCB-FI) test is widely recognized for its great capacity to distinguish the cracking performance of asphalt mixtures [15,20].

During the testing procedure of the SCB-FI and most other SCB tests, a notch was inserted along the symmetry axis of each specimen to produce a stress concentration [21,22]. However, notch cutting is costly and time consuming as well as producing unexpected testing variability. In terms of the fracture toughness of porous asphalt concrete at different temperatures combined with various displacement rates, notched SCB specimens have a larger variance than un-notched specimens [23]. The flexibility index (FI) results of notched specimens show a higher coefficient of variation (COV) than those of un-notched specimens (COV of 13.7%–41.2% versus 8.6%–32.0%) [24]. The higher variability of notched specimens may be owing to the difficulty in maintaining an identical position, width, and depth of the notch for different specimens. In addition, the material properties vary at the notch tip owing to the inhomogeneous characteristics of the asphalt mixtures, which may influence the crack propagation phase. In addition to lower variability, the un-notched SCB test can be employed to describe the complete damage process, including the crack-initiation phase [25]. Additionally, comparing the results of the un-notched and notched SCB tests, a strong linear correlation ($R^2 > 0.95$) exists in their FI values [24]. Therefore, the un-notched SCB test was selected in this study as a reasonable alternative to the conventional notched SCB test.

Several factors can contribute to the cracking performance of asphalt mixtures, including air void, binder performance grade (PG) and content, reclaimed asphalt pavement materials, aging, and environmental conditions [26–30]. Therefore, it is critical to identify and evaluate the factors that significantly affect the cracking performance of asphalt mixtures. Several studies have considered the effects of various factors on the cracking performance of asphalt mixture samples produced in the laboratory [26,31–33]. However, significant differences exist between laboratory-produced and field-cored samples, such as air void, compaction degree, production temperature, and homogeneity [34]. Therefore, it is necessary to determine the effects of various factors on in-service pavements by evaluating the cracking resistance of field-cored samples. Biligiri [35] compared the crack resistance and predicted service life of mixes in common pavement structures used in Sweden with those of mixes in modified pavement systems by utilizing SCB tests. Fang [36] investigated the fracture and fatigue characteristics of field core samples taken from a section of a highway in Jiangsu Province, China by using the SCB test and stereo-DIC. In terms of previous research on the influencing factors on field-cored sample properties, both mixture-design parameters and external conditions were considered for the statistical evaluation of the factors affecting high-temperature performance using the multi-sequenced repeated load test [37]. Significant factors that influence the tensile strength and fracture energy of field cores from the three asphalt layers were determined using low-temperature SCB tests [38,39].

The SCB test is now increasingly used for field core samples, due to its reasonable size, simple operation, and distinguishable index. However, as mentioned above, most of the studies mainly focus on a particular field case, or some laboratory-produced asphalt mixes. There is a lack of systematic studies on asphalt field materials with different service ages, traffic volumes, and material properties. This study uses the SCB test method and its related indexes to characterize the deterioration of the cracking resistance of asphalt field materials under the influence of different internal and external factors and reveal the significant factors affecting different layers of asphalt pavements.

In this study, the fracture potentials of 429 semicircular specimens from three asphalt layers of 16 in-service freeway sections with different structures, traffic loads, and service ages were assessed using the SCB test at 25 °C with a loading rate of 50 mm/min. The FI and tensile strength were chosen as cracking performance indices. Statistical analyses were conducted to verify the influence of material and external factors on the fracture resistance of in-service asphalt pavements.

2. Materials and Methods

2.1. Information about Field-Cored Samples

As shown in Table 1, field cores were drilled from 16 in-service road sections with diverse material properties and external conditions in Jiangsu Province, China. Table 1 lists the key information about the service age, pavement structure, mix type, and cumulative number of equivalent single-axle loads (ESALs) for each road section. The structure of all the sections is an asphalt mixture surface with a semi-rigid base built by cement-stabilized macadam or lime–fly ash macadam, which is the most common freeway structure in Jiangsu Province. The surface layer consists of top, middle, and bottom layers with thicknesses of approximately 4, 6, and 8 cm, respectively. The top and middle layers used the styrene-butadiene-styrene polymer-modified asphalt binder PG70-22 and the bottom layer used neat asphalt.

Table 1. Information about the road sections.

Road Sections	Service Age (Year)	Pavement Structure			ESALs (Million Times/ Lane)	Overload Rate (%)
		Top Layer	Middle Layer	Bottom Layer		
1	4.2	SMA-13 [1]	SUP-20 [2]	SUP-25	2.19	14.10
2	9.2	SMA-13	SUP-20	SUP-25	4.18	13.34
3	9.5	SMA-13	SUP-20	SUP-25	1.69	12.44
4	9.7	SMA-13	SUP-20	SUP-25	2.87	7.88
5	10.4	SMA-13	SUP-20	SUP-25	6.12	16.04
6	10.4	SMA-13	SUP-20	SUP-25	8.88	17.60
7	11.2	SMA-13	SUP-20	SUP-25	2.15	10.05
8	14.1	SMA-13	SUP-20	SUP-25	15.36	9.27
9	14.1	SMA-13	AC-20 [3]	AC-25	10.13	11.10
10	14.1	SMA-13	AC-20	AC-25	25.63	19.15
11	14.8	SMA-13	SUP-20	SUP-25	9.35	14.43
12	17.4	SMA-13	AC-20	AC-25	13.15	15.59
13	17.6	SMA-13	SUP-20	SUP-25	14.65	19.08
14	17.6	SMA-13	SUP-20	SUP-25	18.47	19.20
15	18.1	AK-13 [4]	AC-20	AC-25	25.90	21.68
16	18.6	AK-13	AC-20	AC-25	22.18	18.65

[1] SMA: stone mastic asphalt, [2] SUP: superpave volumetric design criteria, [3] AC: Chinese specifications for the design of highway asphalt pavements [40], [4] AK: a type of coarse-type dense graded asphalt mixture; 13/20/25 is the nominal maximum aggregate size of the mix.

Full-depth core samples of the asphalt surface course in the shape of a cylinder with a height of 18 cm and diameter of 15 cm were drilled at two-wheel tracks as shown in Figure 1. Figure 2a shows the coring procedure of asphalt field samples. The coring of all the sections was completed in the fourth quarter of 2021, with a total of 96 core samples used for this study. A typical core sample with three asphalt layers and a semi-rigid base, the field cores, and semi-circular specimens are shown in Figure 2b–d.

2.2. Testing Procedure

The untreated cylindrical core samples of the asphalt surface course were 150 mm in diameter and 170–180 mm in height. As shown in Figure 3, the top layer was cut according to its actual thickness, generally about 40 mm. The thicknesses of the middle and bottom layers were approximately 60 and 80 mm, respectively, and both were cut into cylinders of 50 mm thickness. The cylinders of all three layers were cut into two semicircles along

the diameter to replicate each other. Nine semicircular specimens were discarded owing to variability in the cutting process, and 429 standard specimens were finally fabricated for subsequent SCB tests.

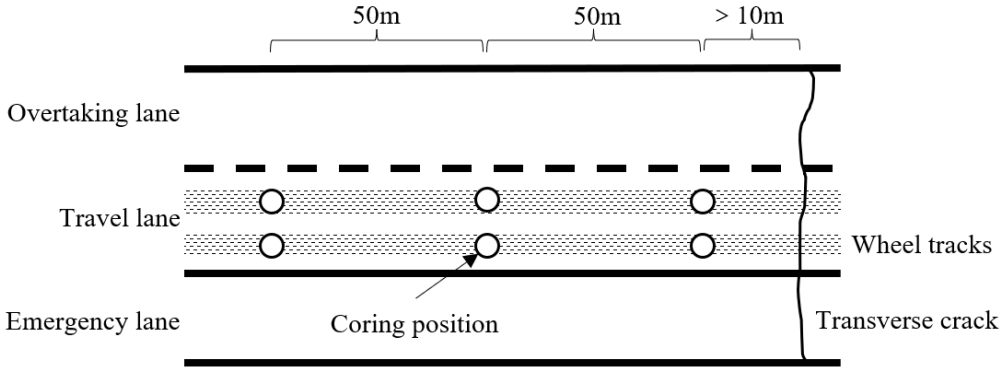


Figure 1. Schematic of coring position.

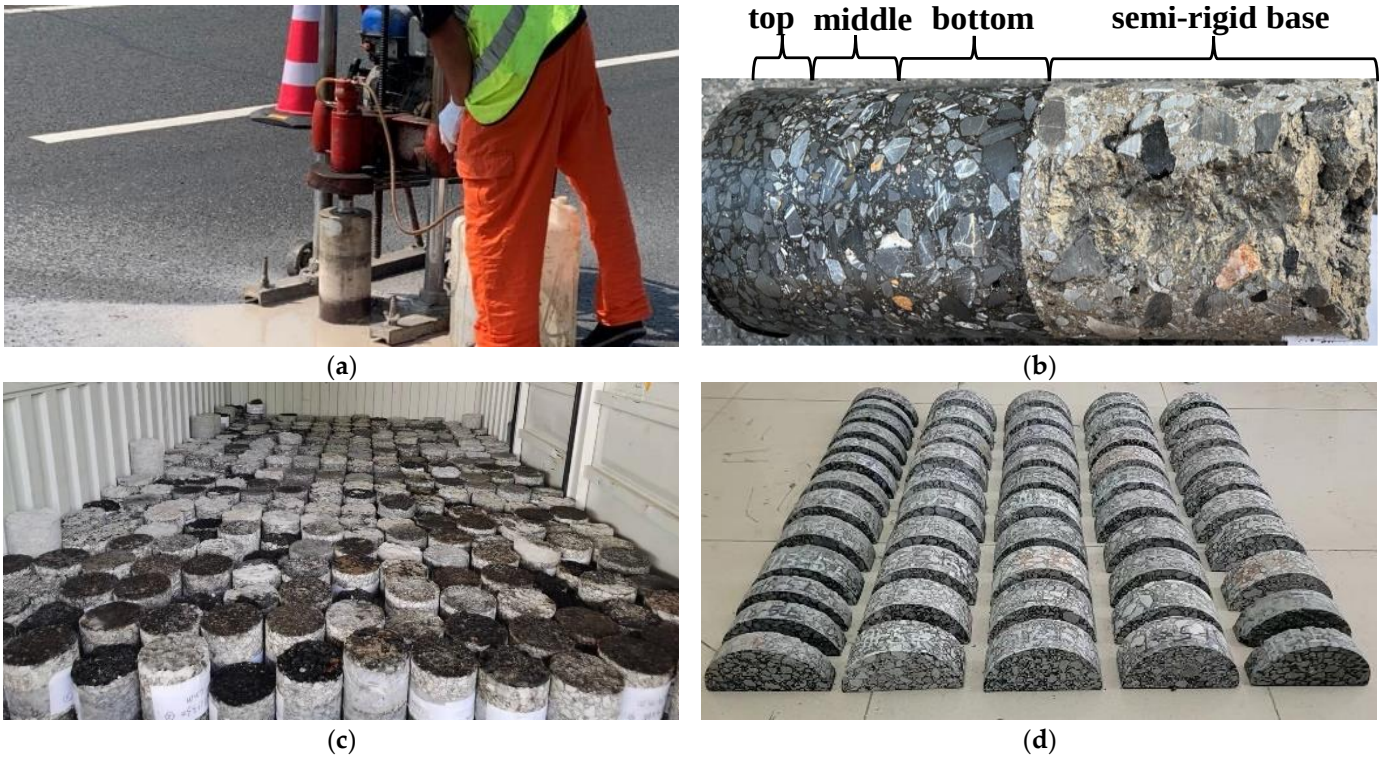


Figure 2. (**a**) Coring procedure; (**b**) A typical field core with three asphalt layers and a semi-rigid base; (**c**) Field cores; (**d**) Semi-circular specimens.

As shown in Figure 4, a UTM-25 (IPC, Melbourne, Australia) universal testing system with a bend test fixture was utilized in this study, which could deliver loads in compression with a resolution of 10 N and maximum capacity of 25 kN. The SCB test was conducted according to AASHTO TP 124 [21]. Figure 4c shows the schematic of the specimen under the SCB test. The distance between the two roller supports at the bottom of the sample is 0.8 times the diameter of the semi-circular specimen, which is 120 mm in this study. The top of the specimen is the load actuator. Before the test, the specimens were kept in an environmental chamber at 25 °C for more than 4 h to ensure that the internal temperature of the specimen also reaches 25 °C, which is the test temperature. The test was conducted using displacement control at a rate of 50 mm/min and the applied load was measured.

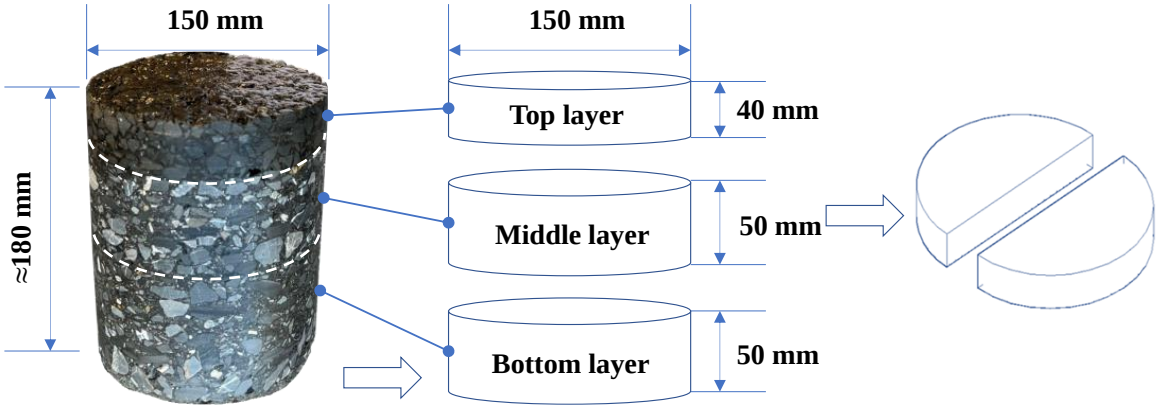
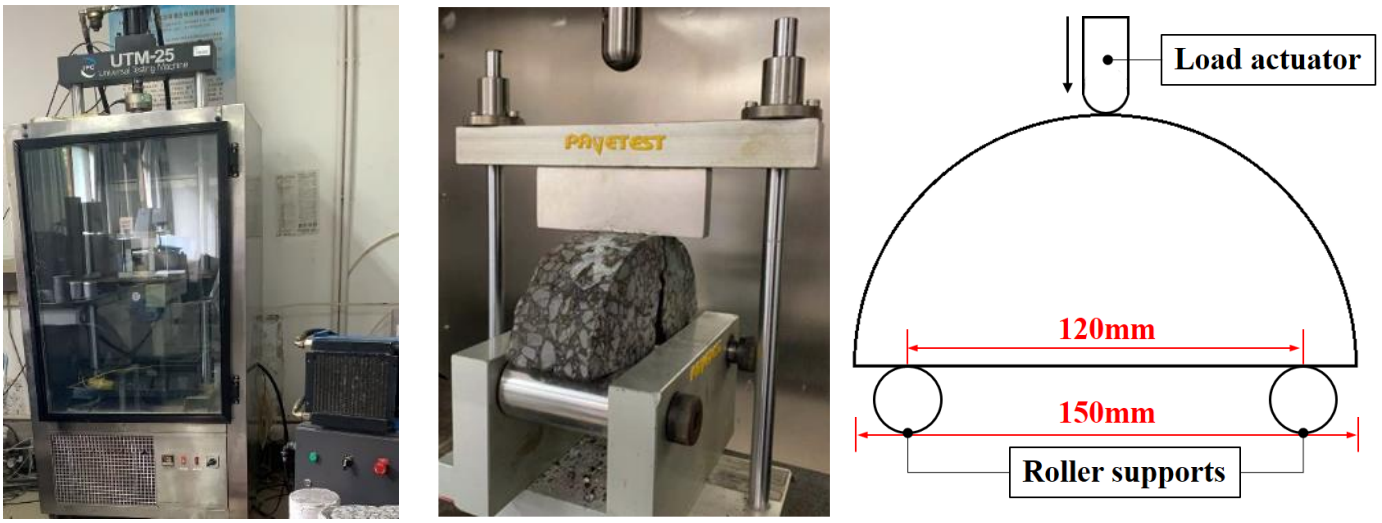


Figure 3. Schematic of SCB specimen preparation for the three asphalt layers.



(**a**) (**b**) (**c**)

Figure 4. (**a**) UTM-25 universal testing system; (**b**) Bend test fixture; (**c**) Specimen under SCB test.

The FI is defined by Equation (1) using the parameters obtained from the load–displacement curve of the SCB test, as shown in Figure 5. A simple correction factor was established to eliminate the effect of thickness variations on the FI, as expressed in Equation (1) [41]. Considered as the evaluation index, the tensile strength (σ_t) of the un-notched SCB specimen geometry was determined using Equation (4) as follows [14]:

$$FI = \frac{G_f}{|m|} \times A \times \frac{B}{50}, \quad (1)$$

$$G_f = \frac{W_f}{A_{lig}} \times 10^6, \quad (2)$$

$$A_{lig} = 0.5 \times B \times D, \quad (3)$$

$$\sigma_t = \frac{4.8 \times F}{B \times D}, \quad (4)$$

where FI denotes the flexibility index, G_f (J/m^2) denotes the fracture energy, and m denotes the slope at the inflection point on the load–displacement curve after the peak point, as shown in Figure 5. A = 0.01 for unit conversion and scaling, B (mm) denotes the specimen thickness, and W_f (J) denotes the work of fracture, calculated as the area under the load–displacement curve using analytical integration. The pre-peak and post-peak load portions of the curve were fitted using a polynomial function and an exponential-based function

before integration, where A_{lig} (mm^2) denotes the ligament area, σ_t (MPa) denotes the tensile strength, F (kN) denotes the peak load, and D (mm) denotes the specimen diameter.

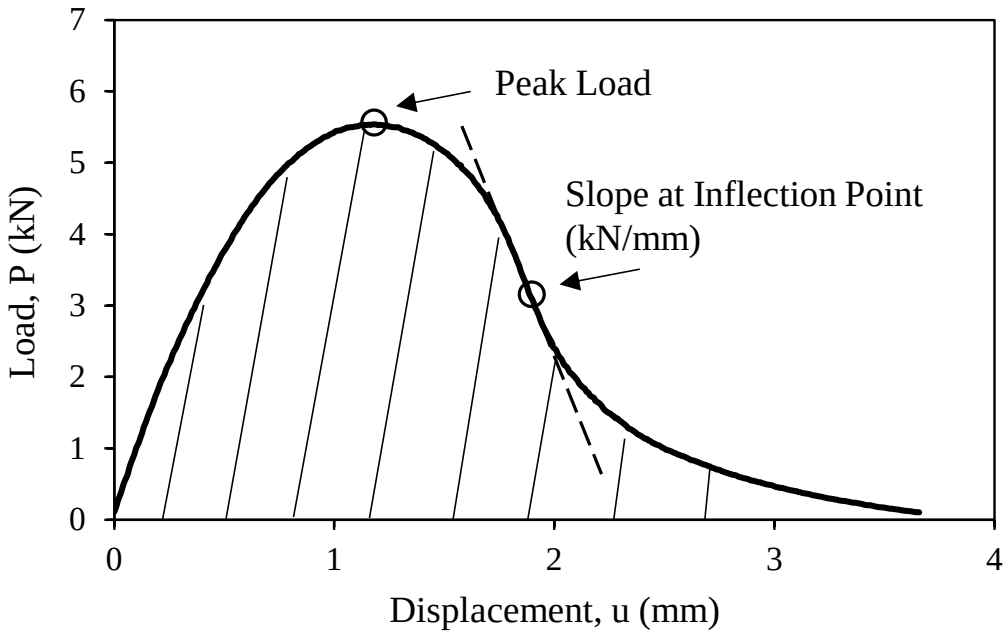


Figure 5. Typical load–displacement curve from the SCB test.

3. Results and Discussion

The distribution of the FI and tensile strength results are shown in Figure 6. In contrast, the tensile strength was much closer to a normal distribution, while the FI was mostly distributed below 10. The specimens with low fracture energy usually have a fast drop in the post-peak load–displacement curve, leading to a low FI value, which is the fracture energy divided by the slope.

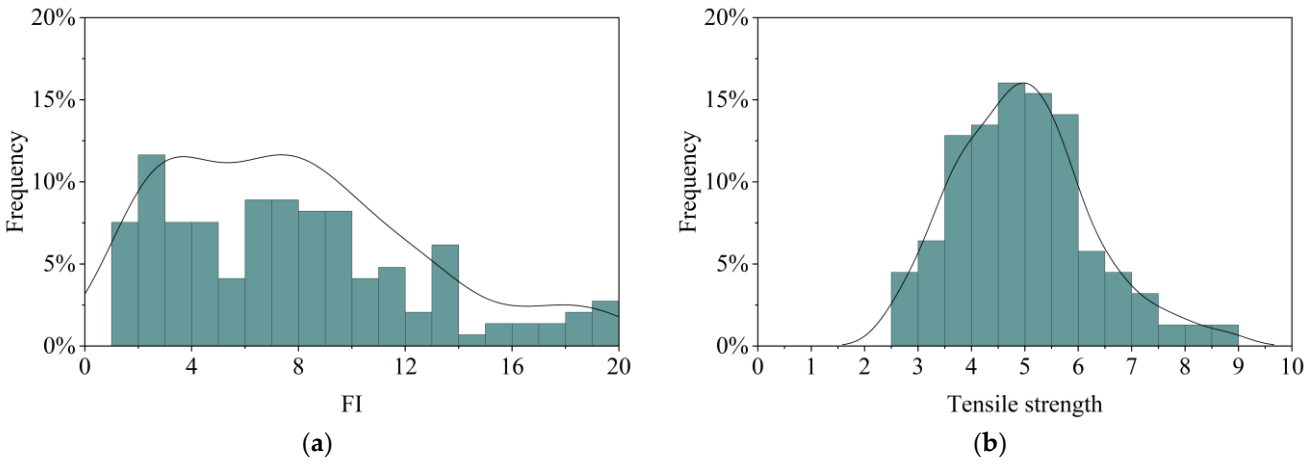


Figure 6. Distribution of (**a**) FI and (**b**) tensile strength.

Analysis of variance (ANOVA) is a valid method used to investigate whether different levels of control variables have significant effects on observation variables. In this study, ANOVA was performed to evaluate the effect of these factors on the cracking resistance of the three asphalt layer samples. A probability value (*p*-value) less than the significance level (0.05) indicated that the factor was statistically significant. The following five factors were considered: air void, mixture type, service age, ESALs, and overload rate. The overload

rate, calculated as the percentage of axle load over 100 kN, ranged from 7.9% to 21.7% for the selected sections, indicating a serious overload problem.

3.1. Effect of Factors on the Top Layer

The ANOVA results for the FI and tensile strength of the top layers are presented in Table 2. In terms of the FI of the top layer, service age and ESALs were significant factors, with *p*-values less than 0.05. Another traffic load indicator, the overload rate, has a *p*-value close to 0.05, indicating that there is a certain effect of different levels of overload on the top layer's FI; however, it is less significant than the ESALs. With regard to tensile strength, only ESALs were a significant factor with a *p*-value less than 0.05. Owing to excessive compaction during construction and axial load, the air void of the top layer samples in this study was low and concentrated (3.4%–4.2%), which had an insignificant effect on the indices. The effects of ESALs and service age on FI, as well as the effect of ESALs on tensile strength, are analyzed in detail below.

Table 2. ANOVA results of indices for the top layer.

Index	Factors	Mean Square	F-Value [1]	*p*-Value [2]	Significance [3]
FI	Air void	1.2114	1.4624	0.2330	N
	Mixture type	0.9256	1.1174	0.2962	N
	Service age	3.5536	4.2899	0.0442 [4]	Y
	ESALs	13.6821	16.5171	0.0002 [4]	Y
	Overload rate	3.1338	3.7832	0.0582	N
Tensile strength	Air void	0.0362	0.0176	0.8953	N
	Mixture type	2.0054	0.9715	0.3304	N
	Service age	6.8863	3.3360	0.0754	N
	ESALs	15.0725	7.3016	0.0101 [4]	Y
	Overload rate	0.2629	0.1274	0.7231	N

[1] F-value, the ratio of mean squares, is used to determine the *p*-value. [2] Factor is significant if the *p*-value < 0.05. [3] Y indicates the factor is significant, while N indicates it is not significant. [4] *p*-value less than 0.05.

Figure 7 presents the detailed relationship between FI and the significant factors for the top layer. As shown in Figure 7a, although some of the data were scattered, the median values of FI declined continuously with increasing ESALs, indicating that there is significant fatigue performance degradation of the pavement material in the field under repeated load.

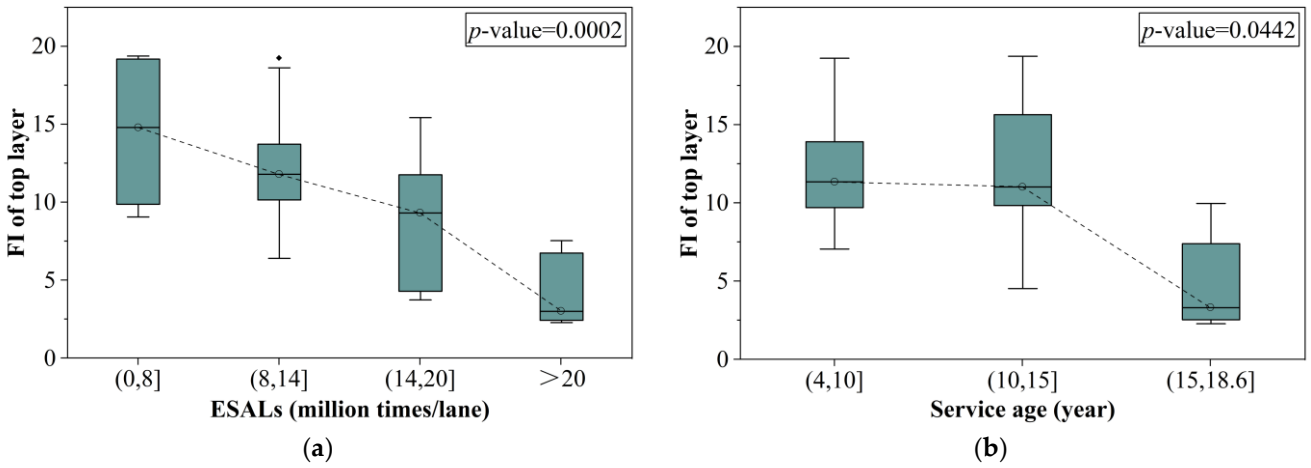


Figure 7. Relationship between FI and significant factors for the top layer: (**a**) FI versus ESALs and (**b**) FI versus service age.

Figure 7b reveals that the FI values of service age less than 15 years were mostly distributed between 9 and 16, while the FI of service age more than 15 years decreased

significantly, with a reduction of about 70% in the median value. This indicates that environmental effects and load accumulation caused the cracking performance of the top layer material to decline sharply after more than 15 years of service.

The accumulation of ESALs is related to both the service age and the traffic level. The decline patterns were compared for samples of similar service age or ESALs to further validate the sensitivity of FI to the effects of service age and traffic level.

Two sample groups aged 14.1–14.8 and 17.4–18.6 years were selected to accurately investigate the relationship between FI and ESALs without the effect of service age. As shown in Figure 8, the FI curve for the 17.4–18.6 years sample consistently lies below the 14.1–14.8 years sample because of the longer service time. The FI of both groups keeps declining with increasing ESALs, while the rate of decline gradually decreases.

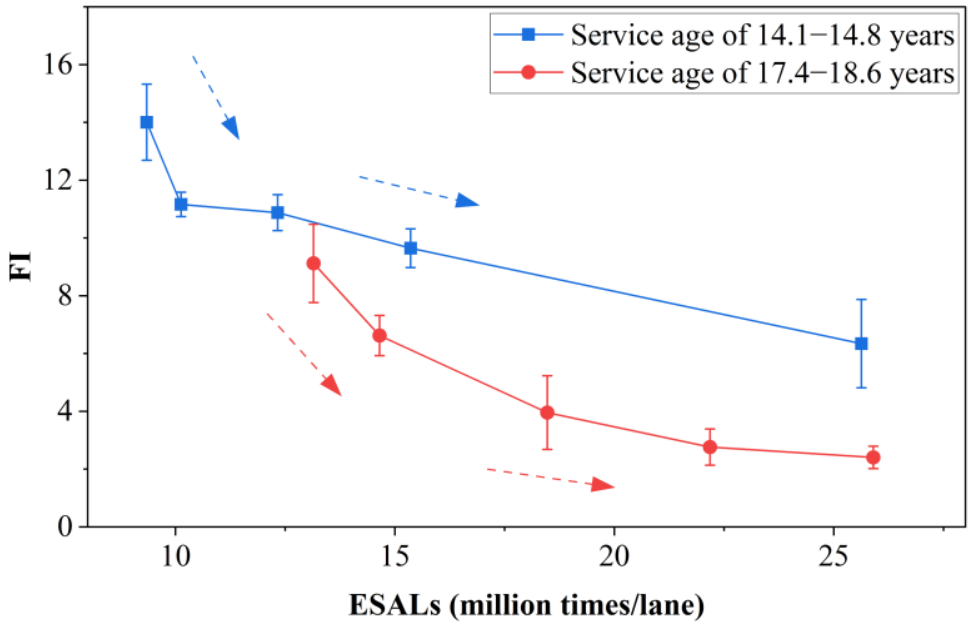


Figure 8. FI versus ESALs for samples of top layer with similar service ages.

In order to investigate the relationship between FI and service age, four groups of samples corresponding to different levels of ESALs were selected. The difference in ESALs within each group was less than one million times/lane to eliminate the effect of ESALs. Information about the four sample groups is shown in Table 3.

Table 3. Information about the four sample groups.

Group	Service Age (Years)	ESALs (Million Times/Lane)	Traffic Level
A	4.2–11.2	2.15–2.19	Light
B	10.4–14.8	8.88–9.35	Medium
C	14.1–17.6	14.65–15.36	Medium
D	14.1–18.1	25.63–25.9	Heavy

As seen in Figure 9, the FI curve of the group with more ESALs always lies below that of the group with fewer ESALs, showing a stepwise decline with age. The small graph in Figure 9 shows the absolute values of the slopes of the FI curves of the four groups, and the slope of Group C is much larger than for the other three groups. Group A and B had a service age of less than 10 years with intact or slightly damaged material in the top layer, so the FI declines the slowest with age. In the first 14 years of service for group D, with a heavy traffic level, the FI value declined to a relatively low level with axle load accumulation. Therefore, the FI of Group D declined more slowly with age than that of Group C, while still faster than that of group A and B because of the higher traffic level and service age.

In contrast, the top layer material of the sections with a medium traffic level represented by Group C showed the most significant decline in crack resistance with age after serving for around 14 years. The most probable reason for this result is that the designed life of expressways in Jiangsu Province is 15 years. For the top layer of the medium-traffic section, its cracking resistance declines slower than that of the heavy-traffic section during the designed life. Therefore, it can be seen in Figure 9 that the cracking resistance of the top layer of Group C is better than that of Group D around the designed life. After exceeding its designed life, the cracking resistance of the top layer of the medium-traffic road section decreases rapidly due to the long-term aging effect in the field.

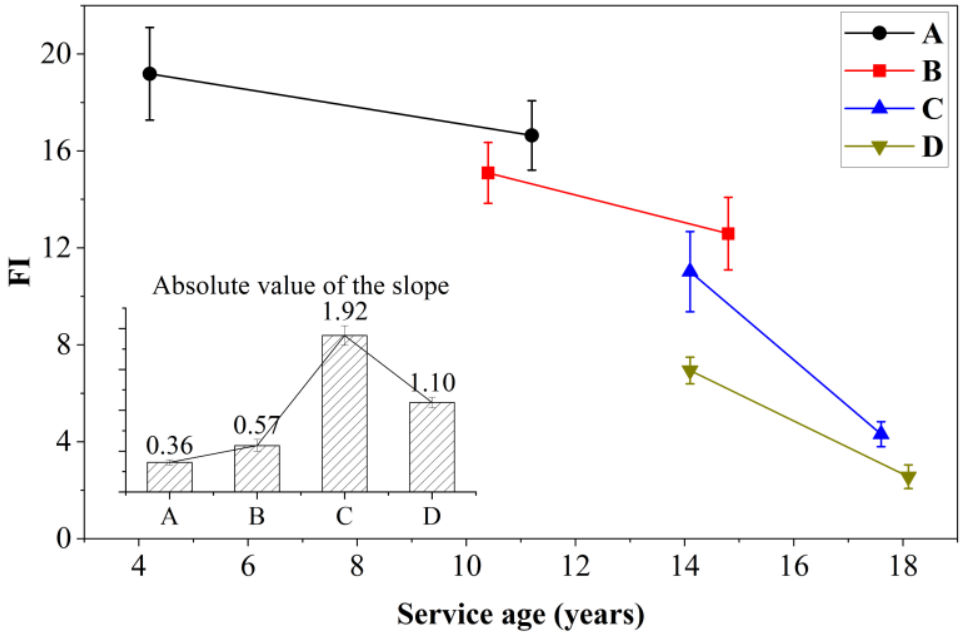


Figure 9. FI versus service age for samples of top layer with similar ESALs.

Figure 10 presents the relationship between tensile strength and ESALs. Compared with FI, the tensile strength declined with increasing ESALs at a much slower rate. From the smallest to the largest ESAL interval, the FI decreased by 79.57%; however, the tensile strength decreased by only 30.19%. Therefore, for the top layer samples, the FI was more sensitive to the ESALs than the tensile strength.

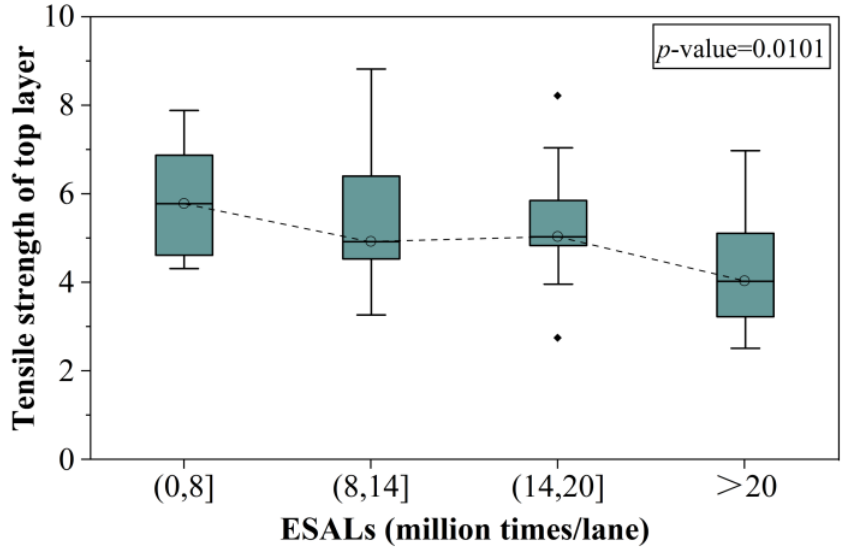


Figure 10. Relationship between tensile strength and ESALs for the top layer.

3.2. Effect of Factors on the Middle Layer

According to the ANOVA results of the FI for the middle layer, the ESALs and overload rate, with *p*-values of 0.0013 and 0.0156, respectively, were significant factors (*p*-values less than 0.05). In contrast to the top layer, service age, with a *p*-value of 0.0696, was not a significant factor affecting crack resistance. In addition, the *p*-values of the air void and mixture type were far beyond the significance level. In terms of tensile strength, only the air void had a *p*-value less than 0.05 (0.0029). The *p*-values of the other factors of tensile strength were significantly higher than 0.05. A particular analysis of the effect of ESALs and overload rate on FI, as well as the effect of air void on tensile strength, is presented below.

The FI of the middle layer showed a decreasing trend with ESALs as seen in Figure 11a. When the ESALs were between 8 and 20 million, the FI decreased slowly with ESALs in a stable period. When the ESALs were greater than 20 million, the median of FI decreased rapidly to 3.69, because the stability of the middle layer was greatly influenced by the development of top-down fatigue cracks under repeated axle load.

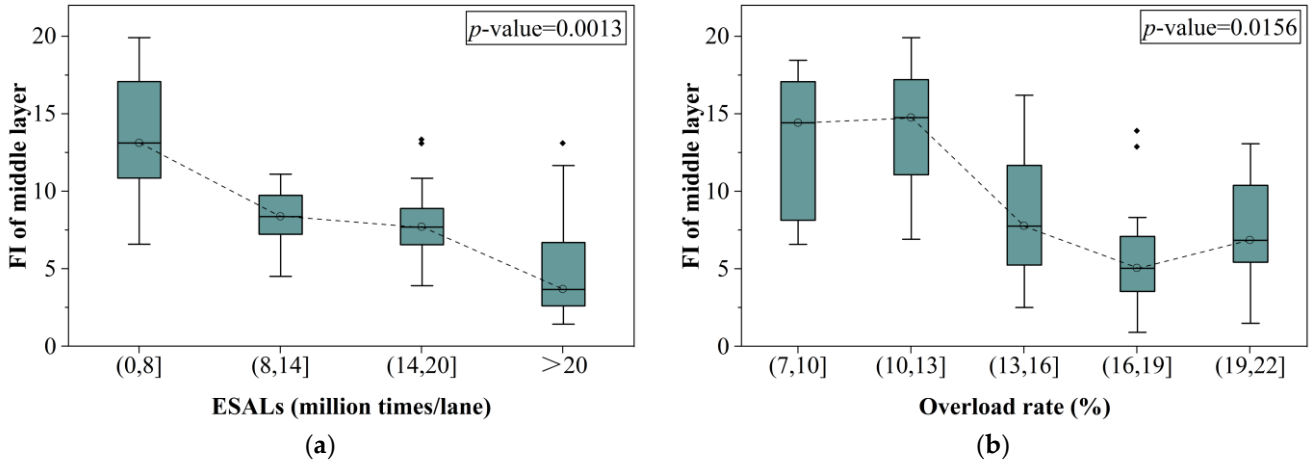


Figure 11. Relationship between FI and significant factors for the middle layer: (**a**) FI versus ESALs and (**b**) FI versus overload rate.

Compared with the top layer, the overload rate replaced service age as a significant factor in the FI of the middle layer. Under the protection of the top layer, the influence of external environmental conditions on the middle layer declined remarkably, weakening the effect of the service age. However, even with the protection of the top layer, a severely overweight axle load may still cause performance degradation. Therefore, for the middle layer, the difference in the overload rate had a more significant impact on FI than service age. According to the relationship between FI and overload rate presented in Figure 11b, although there are some fluctuations, the FI generally decreases as the overload rate increases. When the overload rate was approximately 10%–19%, the FI was highly sensitive to changes in the overload rate. Therefore, the cracking resistance of the middle layer of a heavy-traffic highway section with an overloaded rate over 10% declines faster than that of a light-traffic section with a low overload rate. For this kind of highway section, asphalt overlay is recommended as a maintenance method. The asphalt overlay shifts the original middle layer down in the overall structure of the pavement and slows down its performance degradation.

The air void of the SCB specimens was determined using AASHTO T 166 [42]. This is the only significant factor affecting the tensile strength of the middle layer. According to the correlation relationship displayed in Figure 12, the tensile strength gradually decreased with an increase in air void. The application of the linear fit is based on the relationship between tensile strength and air void found by previous studies [43,44]. This result is consistent with the fact that mixtures with low air void are stiffer than those with high air void, exhibiting a higher peak load and tensile strength in the SCB test [44].

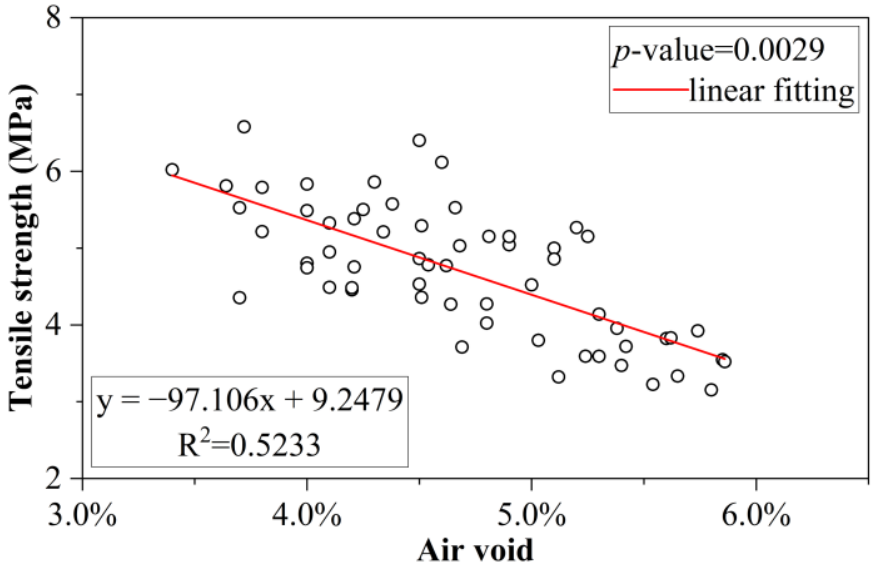


Figure 12. Relationship between tensile strength and air void for the middle layer.

3.3. Effect of Factors on the Bottom Layer

The ANOVA results revealed that the air void was the only significant factor for both the indices of the bottom layer. In addition, the *p*-value of the air void for the tensile strength was significantly smaller than that for the FI (<0.0001 vs. 0.0007). The specific effect of air void on both indices is analyzed below.

Compared with the top and middle layers, the bottom layer had the lowest position on the asphalt pavement surface course, and the environmental and load conditions were relatively tolerant. Therefore, ESALs, service age, and overload rate had slight effects on the performance of the bottom layers, which is consistent with the results of the ANOVA.

Figure 13 illustrates the correlation between the indices and the air void of the bottom layer. Kaseer [26] found a strong linear relationship between the FI and air void, which also existed in other studies [45–47]. Therefore, a linear fit was also performed for the values of FI and air void in this study. The tensile strength decreased with an increase in the air void, which was consistent with the law of the middle layer. However, FI showed an opposite trend. It is well known that more energy is consumed in the crack initiation and propagation phases of denser asphalt mixtures generated with more compaction energy. Therefore, the higher the air void, the lower the fracture energy [47]. Furthermore, the decrease in the peak load owing to the increase in the air void yielded a lower absolute value of m (post-peak slope). When calculating the FI, a decrease in fracture energy will decrease the FI; however, at the same time, a decrease in the absolute value of m will increase the FI with a more dominant effect [26]. Therefore, a tentative air void correction factor was used to adjust FI values based on the air void contents of the samples, as shown in Equation (5) [26]:

$$FI_{4\%} = FI \times \frac{4\%}{AV}, \quad (5)$$

where $FI_{4\%}$ is the corrected FI using 4% as a reference air void and AV is the air void content.

3.4. Summary of Factors Influencing the Three Asphalt Layers

According to the above analysis, the significant factors affecting the cracking resistance of the three asphalt layers are summarized in Table 4. It was found that the cracking performance of the top and middle layers was significantly affected by several factors, including ESALs, service age, overload rate, and air void. However, the bottom layer indices were affected only by air void. Regarding the FIs of the three layers, ESALs had a significant effect on the upper two layers but had no effect on the bottom layer. In addition, regarding the tensile strength, ESALs had a significant effect only on the top layer.

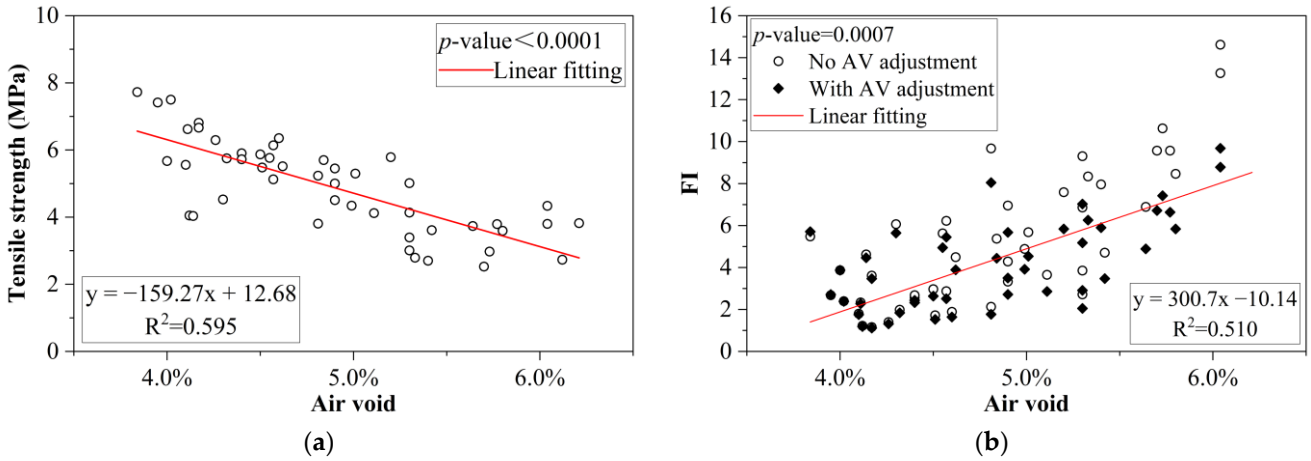


Figure 13. Relationship between significant factors and air void for the bottom layer: (**a**) tensile strength versus air void and (**b**) FI versus air void.

Table 4. Summary of factors affecting the cracking resistance for three asphalt layers.

Layers	Cracking Indices	Significant Factors	*p*-Value
Top	FI	Service age	0.0442
		ESALs	0.0002
	Tensile strength	ESALs	0.0101
Middle	FI	ESALs	0.0013
		Overload rate	0.0156
	Tensile strength	Air void	0.0029
Bottom	FI	Air void	0.0007
	Tensile strength	Air void	<0.0001

A multivariate technique was used to summarize the degree of linear relationship between ESALs and the FIs of the three layers. When an exact linear relationship exists between two variables, the correlation coefficient is 1 for a positive correlation and −1 for a negative correlation. When no linear relationship exists, the correlation coefficient tends to 0. Table 5 lists the correlation coefficient matrix. The degree of linear correlation between ESAL and FI was ranked as follows: top layer > middle layer > bottom layer. This indicates that there is no correlation between ESALs and the FI of the bottom layer because the coefficient is close to 0. The correlation results confirmed that traffic load only affects the crack resistance of the two upper asphalt layers.

Table 5. Multivariate correlations between ESALs and FIs of the three asphalt layers.

Correlation Item	ESALs	FI of Top Layer	FI of Middle Layer	FI of Bottom Layer
ESALs	1	−0.67382	−0.30739	0.03645
FI of top layer	−0.67382	1	0.179072	−0.11837
FI of middle layer	−0.30739	0.179072	1	−0.18856
FI of bottom layer	0.03645	−0.11837	−0.18856	1

The following Table 6 compares the effects of these five factors on cracking resistance at an intermediate temperature revealed by this study and previous studies in recent years. The current results on the effect of air void and mix type are consistent with previous studies. In the past, there was a lack of studies on the effects of external factors on different asphalt layers in the field.

Table 6. Comparison of effects of factors on cracking resistance with previous studies.

Factors	Cracking Resistance at Intermediate Temperature	
	Current Results	Previous Studies
Air void (↑) [1]	FI (↑) Tensile strength (↓) [2]	FI (↑) Tensile strength (↓) [26,38,44,45]
Mixture type	Non-sensitive	Non-sensitive [26,45]
Service age (↑)	↓ (top layer only)	Not found
ESALs (↑)	↓ (not for bottom layer)	Not found
Overload rate (↑)	↓ (middle layer only)	Not found

[1] ↑ indicates an increase in value, [2] ↓ indicates a decrease in value.

4. Conclusions

In this study, the intermediate-temperature cracking resistance of asphalt field mixtures from 16 freeway sections in Jiangsu Province, China was evaluated based on the SCB test. Five material properties and external conditions were considered in the statistical evaluation to reveal significant factors affecting the FI and tensile strength of the three asphalt layers. The key findings of this study are summarized below.

1. Regarding the top asphalt layer, ESALs had a significant effect on both indices, while service age only had a significant effect on FI. The FI declined with increasing ESALs, while the rate of decline gradually decreased. The most rapid decline in crack resistance with age occurred on medium-traffic-level sections that served for over 14 years.
2. For the middle asphalt layer, the FI was significantly affected by ESALs, followed by the overload rate. The FI was highly sensitive to an overload rate of approximately 10%–19%.
3. For the bottom asphalt layer, FI and tensile strength were only affected significantly by the air void.
4. Comparing the five factors, the effect of the traffic load decreased with the depth of the pavement structure. The air void gradually becomes a crucial factor with increasing depth. The current results on the effect of air void and mix type agree with the ones in previous studies. The effect of external factors on the cracking performance of different asphalt layers in the field was revealed, which has rarely been studied in the past.
5. Indicating the overall ductility of the asphalt mixture, the FI was more sensitive to the traffic load than the tensile strength. The tensile strength was more sensitive to the air void as a stiffness index. When the traffic load was a significant factor, both FI and tensile strength decreased as the traffic load increased. When the effect of the air void was dominant, the tensile strength decreased as the air void increased, whereas FI, counterintuitively, exhibited the opposite trend.

This study can be expanded by field samples from a broader array of freeway sections. In addition, it is of interest to establish a correlation between SCB cracking indices and real-world pavement cracking performance data. All these analyses will contribute to further investigations into the effects of various factors on the cracking of long-term-service asphalt pavements.

Author Contributions: Conceptualization, F.N. and D.X.; methodology, D.X., H.D. and Z.Z.; formal analysis, D.X. and H.D.; investigation, D.X., J.W. and S.C.; resources, F.N.; writing—original draft preparation, D.X.; writing—review and editing, H.D. and Z.Z.; supervision, F.N.; funding acquisition, F.N. All authors have read and agreed to the published version of the manuscript.

Funding: This research was funded by Jiangsu Communications Holding Co., Ltd., under several projects (No. 8521009107, No. 8521008990) and a Jiangsu Province Construction System Technology Project (No. 2022ZD099).

Institutional Review Board Statement: Not applicable.

Informed Consent Statement: Not applicable.

Data Availability Statement: All data are included in the article.

Conflicts of Interest: The authors declare no conflict of interest. The funders had no role in the design of the study; in the collection, analyses, or interpretation of data; in the writing of the manuscript; or in the decision to publish the results.

References

1. Lei, G.; Ni, F.; Braham, A.; Luo, H. Mixed-Mode cracking behavior of cold recycled mixes with emulsion using Arcan configuration. *Construct. Build. Mater.* **2014**, *55*, 415–422.
2. Al-Qadi, I.L. Pavement Damage Due to Conventional and New Generation of Wide-Base Super Single Tires. *Tire Sci. Technol.* **2005**, *33*, 210–226. [CrossRef]
3. Saha, G.; Biligiri, K.P. Fracture properties of asphalt mixtures using semi-circular bending test: A state-of-the-art review and future research. *Constr. Build. Mater.* **2016**, *105*, 103–112. [CrossRef]
4. Roque, R.; Buttlar, W.G. Development of a measurement and analysis system to accurately determine asphalt concrete properties using the indirect tensile mode. *Phys. Rev. D Part. Fields* **1992**, *83*, 2235–2239.
5. Kim, Y.R.; Wen, H. Fracture energy from indirect tension testing. *Asph. Paving Technol.* **2002**, *71*, 779–793.
6. Wagoner, M.P.; Buttlar, W.G.; Paulino, G.H. Development of a Single-Edge Notched Beam Test for Asphalt Concrete Mixtures. *J. Test. Eval.* **2005**, *33*, 1–13.
7. Kim, H.; Wagoner, P.M.; Buttlar, W.G. Micromechanical fracture modeling of asphalt concrete using a single-edge notched beam test. *Mater. Struct.* **2008**, *42*, 677–689. [CrossRef]
8. Wagoner, M.; Buttlar, W.; Paulino, G.; Blankenship, P. Investigation of the Fracture Resistance of Hot-Mix Asphalt Concrete Using a Disk-Shaped Compact Tension Test. *Transp. Res. Rec. J. Transp. Res. Board* **2005**, *1929*, 183–192. [CrossRef]
9. Zhou, J.; Scullion, T. *Upgraded Overlay Tester and Its Application to Characterize Reflection Cracking Resistance of Asphalt Mixtures*; FHWA/TX-04/0-4467-1; Texas Transportation Institute: Austin, TX, USA, 2003.
10. Zhou, F.; Sheng, H.; Chen, D.H.; Scullion, T. Overlay Tester: Simple Performance Test for Fatigue Cracking. *Transp. Res. Rec. J. Transp. Res. Board* **2007**, *2001*, 1–8. [CrossRef]
11. Jiménez, F.P.; Vidal, G.V.; Recasens, J.M.; Nieto, R.B. Fenix test: Development of a new test procedure for evaluating cracking resistance in bituminous mixtures. *Transp. Res. Rec. J. Transp. Res. Board* **2010**, *46*, 36–43. [CrossRef]
12. Koh, C.; Lopp, G.; Roque, R. Development of a Dog-Bone Direct Tension Test (DBDT) for Asphalt Concrete. In Proceedings of the 7th International RILEM Symposium on Advanced Testing and Characterisation of Bituminous Materials, Rhodes, Greece, 27 May 2009; pp. 585–596.
13. Zhou, F.; Im, S.; Sun, L.; Scullion, T. Development of an IDEAL Cracking Test for Asphalt Mix Design and QC/QA. *Road Mater. Pavement Des.* **2017**, *18*, 405–427. [CrossRef]
14. Molenaar, A.; Scarpas, A.; Liu, X.; Erkens, S. Semi-Circular Bending Test; Simple but Useful? *Asph. Paving Technol.* **2002**, *71*, 794–815.
15. Ozer, H.; Al-Qadi, I.L.; Lambros, J.; El-Khatib, A.; Singhvi, P.; Doll, B. Development of the fracture-based flexibility index for asphalt concrete cracking potential using modified semi-circle bending test parameters. *Constr. Build. Mater.* **2016**, *115*, 390–401. [CrossRef]
16. Braham, A.; Underwood, S. *State of the Art and Practice in Fatigue Cracking Evaluation of Asphalt Concrete Pavements*; Version 1.0; Association of Asphalt Paving Technologists: Lino Lakes, MN, USA, 2016.
17. Alkuime, H.; Tousif, F.; Kassem, E.; Bayomy, F. Review and evaluation of intermediate temperature monotonic cracking performance assessment testing standards and indicators for asphalt mixes. *Constr. Build. Mater.* **2020**, *263*, 120121. [CrossRef]
18. Sreedhar, S.; Coleri, E.; Haddadi, S.S. Selection of a Performance Test to Assess the Cracking Resistance of Asphalt Concrete Materials. *Constr. Build. Mater.* **2018**, *179*, 285–293. [CrossRef]
19. Elseifi, M.A. Modeling and evaluation of the cracking resistance of asphalt mixtures using the semi-circular bending test at intermediate temperatures. *Road Mater. Pavement Des.* **2012**, *13*, 124–139. [CrossRef]
20. Ozer, H.; Al-Qadi, I.L.; Singhvi, P.; Khan, T.; Rivera-Perez, J.; El-Khatib, A. Fracture Characterization of Asphalt Mixtures with High Recycled Content Using Illinois Semicircular Bending Test Method and Flexibility Index. *Transp. Res. Rec. J. Transp. Res. Board* **2016**, *2575*, 130–137. [CrossRef]
21. *AASHTO TP 124-2018*; Standard Method of Test for Determining the Fracture Potential of Asphalt Mixtures Using the Flexibility Index Test (FIT). American Association of State Highway and Transportation Officials: Washington, DC, USA, 2018.
22. Zhou, Z.; Gu, X.; Ni, F.; Li, Q.; Ma, X. Cracking Resistance Characterization of Asphalt Concrete Containing Reclaimed Asphalt Pavement at Intermediate Temperatures. *Transp. Res. Rec. J. Transp. Res. Board* **2017**, *2633*, 46–57. [CrossRef]
23. Molenaar, J.M.M. Performance Related Characterisation of the Mechanical Behavior of Asphalt Mixtures. Ph.D. Thesis, Delft University of Technology, Delft, The Netherlands, 2003.
24. Yan, C.; Zhang, Y.; Bahia, H.U. Comparison between SCB-IFIT, un-notched SCB-IFIT and IDEAL-CT for measuring cracking resistance of asphalt mixtures. *Constr. Build. Mater.* **2020**, *252*, 119060. [CrossRef]
25. Jiang, J.; Dong, Q.; Ni, F.; Zhao, Y.J. Effects of Loading Rate and Temperature on Cracking Resistance Characteristics of Asphalt Mixtures Using Nonnotched Semicircular Bending Tests. *J. Test. Eval.* **2019**, *47*, 4. [CrossRef]
26. Kaseer, F.; Yin, F. Development of an index to evaluate the cracking potential of asphalt mixtures using the semi-circular bending test. *Constr. Build. Mater.* **2018**, *167*, 286–298. [CrossRef]

27. Kim, S.S.; Yang, J.J.; Etheridge, R.A. Effects of mix design variables on flexibility index of asphalt concrete mixtures. *Int. J. Pavement Eng.* **2020**, *21*, 1275–1280. [CrossRef]
28. Hanz, A.; Dukatz, E.; Retake, G. Use of Performance Based Testing for High RAP Mix Design and Production Monitoring. *Asph. Paving Technol.* **2016**, *85*, 449–483. [CrossRef]
29. Zhu, Z.; Singhvi, P.; Espinoza-Luque, A.F.; Ozer, H.; Al-Qadi, I.L. Influence of mix design parameters on asphalt concrete aging rate using I-FIT specimens. *Constr. Build. Mater.* **2019**, *200*, 181–187. [CrossRef]
30. Brown, E.R. *Hot Mix Asphalt Materials Mixture Design, and Construction*; National Asphalt Pavement Association Research and Education Foundation: Lanham, MD, USA, 2009.
31. Sreedhar, S.; Coleri, E. The effect of long-term aging on fatigue cracking resistance of asphalt mixtures. *Int. J. Pavement Eng.* **2020**, *23*, 308–320. [CrossRef]
32. Jahangiri, B.; Majidifard, H.; Meister, J.; Buttlar, W.G. Performance Evaluation of Asphalt Mixtures with Reclaimed Asphalt Pavement and Recycled Asphalt Shingles in Missouri. *Transp. Res. Rec. J. Transp. Res. Board* **2019**, *2673*, 036119811982563. [CrossRef]
33. Batioja-Alvarez, D.; Lee, J.; Haddock, J.E. Understanding the Illinois Flexibility Index Test (I-FIT) using Indiana Asphalt Mixtures. *Transp. Res. Rec. J. Transp. Res. Board* **2019**, *2673*, 036119811984128. [CrossRef]
34. Koek, B.V.; Yilmaz, M.; Alatas, T.J. Evaluation of the Mechanical Properties of Field- and Laboratory-Compacted Hot-Mix Asphalt. *J. Mater. Civ. Eng.* **2014**, *26*, 9.
35. Biligiri, K.P.; Said, S.; Hakim, H.J. Asphalt mixtures' crack propagation assessment using semi-circular bending tests. *Int. J. Pavement Res. Technol.* **2012**, *5*, 209–217.
36. Yuan, F.; Cheng, L.; Shao, X.; Dong, Z.; He, X.J. Full-field Measurement and Fracture and Fatigue Characterizations of Asphalt Concrete based on the SCB Test and Stereo-DIC. *Eng. Fract. Mech.* **2020**, *235*, 107127. [CrossRef]
37. Zhao, Z.; Jiang, J.; Ni, F. Factors Affecting the Rutting Resistance of Asphalt Pavement Based on the Field Cores Using Multi-Sequenced Repeated Loading Test. *Constr. Build. Mater.* **2020**, *253*, 118902. [CrossRef]
38. Du, H.; Ni, F.; Zhao, Y. Characterization of the Influence Factors of Low-Temperature Fracture Properties for Serving Asphalt Pavements Using Layer Core Samples. *J. Transp. Eng. Part B-Pavements* **2021**, *147*, 04021016. [CrossRef]
39. Du, H.; Ni, F.; Ma, X. Crack Resistance Evaluation for In-Service Asphalt Pavements by Using SCB Tests of Layer-Core Samples. *J. Mater. Civ. Eng.* **2021**, *33*, 04020418. [CrossRef]
40. *JTG E20-2011*; Standard Test Methods of Bitumen and Bituminous Mixtures for Highway Engineering. Research Institute of Highway Ministry of Transport: Beijing, China, 2011.
41. Al-Qadi, I.; Ozer, H.; Lambros, J.; El Khatib, A.; Singhvi, P.; Khan, T.; Rivera, J.; Doll, B. *Testing Protocols to Ensure Performance of High Asphalt Binder Replacement Mixes Using RAP and RAS*; Report No. FHWA-ICT-15-017; Illinois Center for Transportation: Urbana, IL, USA, 2015.
42. *AASHTO T 166-2013*; Standard Method of Test for Bulk Specific Gravity (Gmb) of Compacted Hot Mix Asphalt (HMA) Using Saturated Surface-Dry Specimens. American Association of State Highway and Transportation Officials: Washington, DC, USA, 2013.
43. Li, X.J.; Marasteanu, M.O. Using Semi Circular Bending Test to Evaluate Low Temperature Fracture Resistance for Asphalt Concrete. *Exp. Mech.* **2010**, *50*, 867–876. [CrossRef]
44. Chen, X.; Solaimanian, M.J. Simple Indexes to Identify Fatigue Performance of Asphalt Concrete. *J. Test. Eval.* **2020**, *48*, 3999–4015. [CrossRef]
45. Majidifard, H.; Jahangiri, B.; Rath, P.; Buttlar, W.G. Development of a Balanced Cracking Index for Asphalt Mixtures Tested in Semi-Circular Bending with Load-LLD. *Measurement* **2020**, *173*. [CrossRef]
46. Riveraperez, J.J. *Effect of Specimen Geometry and Test Configuration on the Fracture Process Zone for Asphalt Materials*; University of Illinois at Urbana-Champaign: Urbana, IL, USA, 2017.
47. Barry, M.K. *An Analysis of Impact Factors on the Illinois Flexibility Index Test*; University of Illinois at Urbana-Champaign: Urbana, IL, USA, 2016.

Disclaimer/Publisher's Note: The statements, opinions and data contained in all publications are solely those of the individual author(s) and contributor(s) and not of MDPI and/or the editor(s). MDPI and/or the editor(s) disclaim responsibility for any injury to people or property resulting from any ideas, methods, instructions or products referred to in the content.